Parameter effects on convergence Meshless Method by using Radial Basis Functions

Jaouad EDDAOUDY*[1], Touria BOUZIANE[2]

Abstract— The numerical solution of partial differential equations (PDEs) resulting of physic problem formulations need appropriate approximation methods. The Point Interpolation Local Radial Method (LRPIM) is a recent numerical meshless method for solving PDEs. It is derived from the local weak form (WF) of the equilibrium equations. Radial Basis Functions (RBFs) are used as a trial function and a cubic spline functions are used as a test function of weighted residual method. In this paper, we present a study of a 2D problem of an elastostatic homogenous rectangular plate by using the LRPIM method. The numerical results are discussed in function of different regular distributions of nodes and by using different radial basis functions RBFs: Multi-quadrics (MQ) and Thin Plate Spline (TPS). In this study, we come to the result that the effect of size parameters of subdomain and the specific parameters of RBFs basis are performed on the accuracy and convergence of the LRPIM method. Interesting numerical results are found and are identical with analytical solution.

Index Terms— Meshless method, Local Radial Point Interpolation Method, Radial basis functions, shape parameters, elastostatic plate.

1 Introduction

Numerical methods are indispensable for the successful simulation of physical problems, as the partial differential equations usually have to be approximated.

Groups of meshfree methods have been developed to accomplish this task, such as Smooth Particle Hydrodynamics (SPH) method [1] in 1977 by Lucy and al., Diffuse Element Method (DEM) [2] in 1992 by Nayroles and al., Element Free Galerkin (EFG) method [3] in 1994 by Belytschko and al.. In 1998 and 2001, Atluri and al. presented six Meshless Local Petrov–Galerkin methods (MLPG) based on different test functions [4],[5]. The Point Interpolation Method (PIM) [6]-[9] is a meshfree method developed using Galerkin weak form and shape functions that are constructed based only on a group of nodes regularly distributed in a local support domain by means of interpolation. Radial Basis Functions (RBF) [10], [11] were first applied to solve partial differential equations in 1990 by Kansa[12], [13] when a technique based on the direct Collocation method and the Multiquadric RBF was used to model fluid dynamics problems. The direct Collocation procedure used by Kansa is relatively simple to implement; however, it results in an asymmetric system of equations due to the mix of governing equations and boundary conditions. The LRPIM approximation [14] using radial basis functions (RBFs) is based on MFree local Petrov Galerkin weak-form methods [15]-[17]. The major advantage of PIM is that the shape functions created possess the Kronecker delta function property, which allows simple enforcement of essential boundary conditions.

*Jaouad EDDAOUDY, j.eddaoudy@edu.umi.ac.ma, jaoaudeddaoudy@gmail.com

[1,2] Department of physic Moulay Ismail University Meknes,

This paper proposes a numerical study of 2D elastostatic prob lem by using LRPIM based on RBF functions. We choose Multi-quadrics (MQ) RBF [10], [11] (this function depends on two shape parameters αc and q) and thin plate spline (TPS) RBF [18] (it has one shape parameter η). The choice of shape parameters functions will affect the performance of LRPIM. The numerical performances of this method are investigated through different numerical values. In Section 2, the local weak form developed using weighted residual method locally from the partial differential equation. In Section 3, the radial basis function (RBF) used to develop the Local radial point interpolation method (LRPIM) shape functions for Mfree weak-form methods. Numerical results and discussion are presented in Section 4 to estimate the accuracy and efficiency of the LRPIM. The conclusion is given in Section 5.

2 Local Radial Point Interpolation Method (LRPIM) formulation

We consider the following two-dimensional static problem, in linear elasticity on the domain Ω bounded by the boundary Γ

$$\begin{aligned} \sigma_{ij,j} + b_i &= 0 && \text{in } \Omega \\ u_i &= \bar{u}_i && \text{at } \Gamma_u \\ \sigma_{ij} n_j &= \bar{t}_i && \text{at } \Gamma_t \end{aligned} \tag{1}$$

Where
σ_{ij}: is the stress tensor,
b_i: the body force,
$\bar{u_i}$: the prescribed displacements on essential boundary Γ_u,
$\bar{t_i}$: the tractions on natural boundary Γ_t,
n_j: the direction index.
The local weighted residual form defined over a local quadrature domain Ωq bounded by Γ_q for a field node I has the following form:

$$\int_{\Omega_q} \theta_I \left(\sigma_{ij,j} + b_i \right) d\Omega = 0 \tag{2}$$

Where θ_I is the weight or test function centered usually at node I.

Using $\sigma_{ij,j}\theta_l = (\sigma_{ij}\theta_l)_{,j} - \sigma_{ij}\theta_{l,j}$ and the divergence theorem [22], we have

$$\int_{\partial\Omega_q} \theta_l \sigma_{ij} n_j \, d\Gamma - \int_{\Omega_q} \theta_{l,j}\sigma_{ij} \, d\Omega + \int_{\Omega_q} \theta_l b_i \, d\Omega = 0 \quad (3)$$

The boundary $\partial\Omega_q$ for the local quadrature domain Ω_q is composed of three parts (see fig.1).

$$\partial\Omega_q = \Gamma_{qi} \cup \Gamma_{qt} \cup \Gamma_{qu} \quad (4)$$

Where
Γqi: the internal boundary of the quadrature domain, which does not intersect with the global boundary Γ,
Γqt: the part of the natural boundary that intersects with the quadrature domain,
Γqu: the part of the essential boundary that intersects with the quadrature domain.
Therefore, Eq. (3) can be re-written as:

$$\int_{\Gamma_{qi}} \theta_l \sigma_{ij} n_j \, d\Gamma + \int_{\Gamma_{qt}} \theta_l \sigma_{ij} n_j \, d\Gamma + \int_{\Gamma_{qu}} \theta_l \sigma_{ij} n_j \, d\Gamma$$

$$- \int_{\Omega_q} \theta_{l,j}\sigma_{ij} \, d\Omega + \int_{\Omega_q} \theta_l b_i \, d\Omega = 0 \quad (5)$$

For a local quadrature domain located entirely within the global domain, there is no intersection between Γq and the global boundary Γ, thus, in this case

$$\partial\Omega_q = \Gamma_{qi} = \Gamma_q$$

There is no integral over Γ_{qu} and Γ_{qt}

$$\int_{\Gamma_q} \theta_l \sigma_{ij} n_j \, d\Gamma - \int_{\Omega_q} \theta_{l,j}\sigma_{ij} \, d\Omega + \int_{\Omega_q} \theta_l b_i \, d\Omega = 0 \quad (6)$$

Considering the relation between the stress and the traction on the boundary

$$\sigma_{ij} n_j = t_i$$

The local weak form Eq. (6) is leading to local boundary integral equations:

$$\int_{\Gamma_q} \theta_l t_i \, d\Gamma - \int_{\Omega_q} \theta_{l,j}\sigma_{ij} \, d\Omega + \int_{\Omega_q} \theta_l b_i \, d\Omega = 0 \quad (7)$$

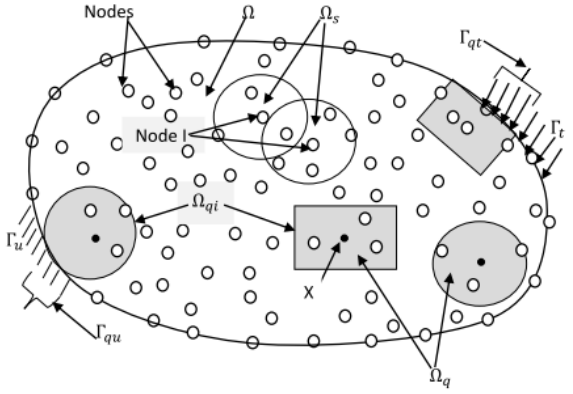

Fg. 1: The local sub-domains around point X and boundaries

3 Point Interpolation using Radial Basis Functions

We consider a point $X^T = (x, y)$ in the local support domain and the continuous function u defined on the problem domain. We use a field number of nodes: *n* in the local support domain to approximate the value $\mathbf{u}^h(X)$ at the point X of function u in the form:

$$\mathbf{u}^h(X) = \sum_{i=1}^{n} R_i(X)\, a_i = \mathbf{R}^T(X)\mathbf{a} \quad (8)$$

Where
n: the number of nodes in the local support domain.
a: the vector of coefficients defined by

$$\mathbf{a}^T = \{a_1, a_2, a_3, \ldots, a_n\} \quad (9)$$

$\mathbf{R}_i(X)$: the Radial basis function it is expressed as

$$R_i(X) = R_i(r_i) = R_i(x, y) \quad (10)$$

ri: the distance between point X= (*x*, *y*) and node (x_i, y_i) in a two dimensional problem

$$r_i = [(x - x_i)^2 + (y - y_i)^2]^{\frac{1}{2}} \quad (11)$$

The vector **R** has the form

$$\mathbf{R}^T(X) = [R_1(X), R_2(X), \ldots, R_n(X)] \quad (12)$$

We used the following radial basis functions:

TABLE I
TYPICAL RADIAL BASIS FUNCTIONS WITH DIMENSIONLESS SHAPE PARAMETERS

Name	Expression	Shape parameters (real number)
1.Multiquadratic(MQ)	$R_i(x,y)=(r_i^2+(\alpha_c d_c)^2)^q$	$\alpha_c \geq 0$, q
2.Thinplatespline(TPS)	$R_i(x,y) = r_i^\eta$	η

The coefficients a_i in Eq. (8) are determined by enforcing the interpolated function u through all the n nodes within the support domain.
The numerical value at the k^{th} point of the function u has the following form:

$$u_k(r_k) = \sum_{i=1}^{n} R_i(x_k, y_k) a_i \qquad k = 1,2 \dots n \qquad (13)$$

with

$$r_k = [(x_k - x_i)^2 + (y_k - y_i)^2]^{\frac{1}{2}} \qquad (14)$$

Eq. (8) can be expressed in matrix form as follows:

$$\mathbf{U} = \mathbf{R_0 a} \qquad (15)$$

Where **U** is the vector that collects all the field nodal variables of u at the n nodes of the support domain, a unique solution for vector of coefficients **a** is obtained if the inverse of $\mathbf{R_0}$ exists:

$$\mathbf{a} = \mathbf{R_0^{-1} U} \qquad (16)$$

Substituting the foregoing equation into Eq. (8) leads to

$$\mathbf{u^h(X)} = \sum_{i=1}^{n} R_i(X) a_i = \mathbf{R^T(X) R_0^{-1} U} = \mathbf{\Phi(X) U} \qquad (17)$$

Where Φ(X) is the matrix of n shape functions

$$\mathbf{\Phi(X)} = [R_1(X), R_2(X), R_3(X) \dots, R_n(X)]\mathbf{R_0^{-1}} \qquad (18)$$

$$= [\varphi_1(X), \varphi_2(X), \dots, \varphi_k(X), \dots, \varphi_n(X)]$$

Approximation for the displacement at a point X is

$$\mathbf{u^h}_{(2\times1)}(X) = \begin{Bmatrix} u \\ v \end{Bmatrix} = \begin{bmatrix} \varphi_1 & 0 & \dots & \varphi_n & 0 \\ 0 & \varphi_1 & \dots & 0 & \varphi_n \end{bmatrix} \begin{Bmatrix} u_1 \\ v_1 \\ \vdots \\ u_n \\ v_n \end{Bmatrix}$$

$$\mathbf{u^h}_{(2\times1)}(X) = \mathbf{\Phi}_{(2\times2n)}(X)\mathbf{U}_{(2n\times1)} \qquad (19)$$

It can also be written in the following form of nodal summation:

$$\mathbf{u^h}_{(2\times1)}(X) = \sum_{I}^{n} \Phi_I \, U_I \qquad (20)$$

Where Φ_I is the matrix of shape functions of node I, and U_I is the nodal displacements.
The strains can be obtained by using the approximated displacement

$$\boldsymbol{\varepsilon}_{(3\times1)} = \mathbf{L u^h} = \mathbf{L}_{(3\times2)} \mathbf{\Phi}_{(2\times2n)} \mathbf{u^h}_{(2n\times1)}$$

$$\boldsymbol{\varepsilon}_{(3\times1)} = \begin{bmatrix} \frac{\partial}{\partial x} & 0 \\ 0 & \frac{\partial}{\partial y} \\ \frac{\partial}{\partial y} & \frac{\partial}{\partial x} \end{bmatrix} \begin{bmatrix} \varphi_1 & 0 & \dots & \varphi_n & 0 \\ 0 & \varphi_1 & \dots & 0 & \varphi_n \end{bmatrix} \begin{Bmatrix} u_1 \\ v_1 \\ \vdots \\ u_n \\ v_n \end{Bmatrix}$$

$$\boldsymbol{\varepsilon}_{(3\times1)} = \begin{bmatrix} \frac{\partial \varphi_1}{\partial x} & 0 & \dots & \frac{\partial \varphi_n}{\partial x} & 0 \\ 0 & \frac{\partial \varphi_1}{\partial y} & \dots & 0 & \frac{\partial \varphi_n}{\partial y} \\ \frac{\partial \varphi_1}{\partial y} & \frac{\partial \varphi_1}{\partial x} & \dots & \frac{\partial \varphi_n}{\partial y} & \frac{\partial \varphi_n}{\partial x} \end{bmatrix} \begin{Bmatrix} u_1 \\ v_1 \\ \vdots \\ u_n \\ v_n \end{Bmatrix}$$

$$\boldsymbol{\varepsilon}_{(3\times1)} = \mathbf{B}_{(3\times2n)} \mathbf{U}_{(2n\times1)} \qquad (21)$$

Where **B** is the strain matrix.
The stress vector using the constitutive equations for the material at the point X in the problem domain can be written as:

$$\boldsymbol{\sigma}_{(3\times1)} = \mathbf{D}_{(3\times3)} \boldsymbol{\varepsilon}_{(3\times1)} = \mathbf{D}_{(3\times3)} \mathbf{B}_{(3\times2n)} \mathbf{U}_{(2n\times1)} \qquad (22)$$

$$\boldsymbol{\sigma}_{(3\times1)} = \sum_{I}^{n} \mathbf{D}_{(3\times3)} (\mathbf{B}_I)_{(3\times2n)} (\mathbf{U}_I)_{(2n\times1)} \qquad (23)$$

For an isotropic homogeneous material in the plane stress state, the matrix of material elastic constants **D** can be expressed as:

$$\mathbf{D} = \frac{E}{1-\nu^2} \begin{bmatrix} 1 & \nu & 0 \\ \nu & 1 & 0 \\ 0 & 0 & \frac{1-\nu}{2} \end{bmatrix} \qquad (24)$$

The traction **t** at a point X has the following form

$$\mathbf{t} = \begin{Bmatrix} t_x \\ t_y \end{Bmatrix} = \begin{bmatrix} n_x & 0 & n_y \\ 0 & n_y & n_x \end{bmatrix} \begin{Bmatrix} \sigma_{xx} \\ \sigma_{yy} \\ \tau_{xy} \end{Bmatrix}$$

$$\mathbf{t} = \mathbf{N}_{(2\times3)} \mathbf{D}_{(3\times3)} \mathbf{B}_{(3\times2n)} \mathbf{U}_{(2n\times1)} \qquad (25)$$

In which (n_x, n_y) is the vector of the unit outward normal on the boundary.
We now change Eq. (7) to the following matrix form to derive the discretized system equations in a matrix form

$$\int_{\Omega_q} \mathbf{W_I}^T \boldsymbol{\sigma} \, d\Omega - \int_{\Gamma_q} \mathbf{\Theta_I}^T \mathbf{t} \, d\Gamma = \int_{\Omega_q} \mathbf{\Theta_I}^T \mathbf{b} \, d\Omega \qquad (26)$$

Where **Θ** is a matrix of weight functions given by:

$$\mathbf{\Theta_I} = \mathbf{\Theta}(X, X_I)_{(2\times2)} = \begin{bmatrix} \theta(X, X_I) & 0 \\ 0 & \theta(X, X_I) \end{bmatrix} \qquad (27)$$

$\mathbf{W_I}$ is a matrix that collects the derivatives of the weight functions

$$W_I = W_I \quad (X, X_I)_{(3\times 2)} = \begin{bmatrix} \theta_x(X, X_I) & 0 \\ 0 & \theta_{xy}(X, X_I) \\ \theta_{xy}(X, X_I) & \theta_x(X, X_I) \end{bmatrix} \tag{28}$$

Substitution of Eqs. (22) and (25) into Eq. (26) leads to the following discretized system of equations for the I[th] field node

$$\int_{\Omega_q} \mathbf{W_I}^T \mathbf{DBU}\, d\Omega - \int_{\Gamma_q} \mathbf{\Theta_I}^T \mathbf{NDBU}\, d\Gamma = \int_{\Omega_q} \mathbf{\Theta_I}^T \mathbf{b}\, d\Omega \tag{29}$$

The matrix form of Eq. (29) can be written as:

$$(\mathbf{K_I})_{2\times 2n}(\mathbf{U})_{2n\times 1} = (\mathbf{F_I})_{(2\times 1)} \tag{30}$$

U is the vector that collect displacements at I[th] node for the field nodes included in the considered support domain,

The matrix $\mathbf{K}_I$ is called nodal stiffness matrix for the I[th] field node, which is computed by using

$$\mathbf{K_I} = \int_{\Omega_q} \mathbf{W_I}^T \mathbf{DB}\, d\Omega - \int_{\Gamma_q} \mathbf{\Theta_I}^T \mathbf{NDB}\, d\Gamma \tag{31}$$

The nodal force vector FI with contributions from body forces applied in the problem domain

$$\mathbf{F_I} = \int_{\Omega_q} \mathbf{\Theta_I}^T \mathbf{b}\, d\Omega \tag{32}$$

Eq. (30) presents two linear equations for the I[th] field node. Using Eq. (30) for all the n_t field nodes in the entire problem domain, we obtain a total of 2nt independent linear equations. Assemble all these 2nt equations based on the global numbering system to obtain the final global system equations in the form:

$$\begin{bmatrix} K_{11} & K_{12} & \cdots & K_{1(2n_t-1)} & K_{1(2n_t)} \\ \vdots & \vdots & \ddots & \vdots & \vdots \\ K_{(2I-1)1} & K_{(2I-1)2} & \cdots & K_{(2I-1)(2n_t-1)} & K_{(2I-1)(2n_t)} \\ K_{(2I)1} & K_{(2I)2} & \cdots & K_{(2I)(2n_t-1)} & K_{(2I)(2n_t)} \\ \vdots & \vdots & \ddots & \vdots & \vdots \\ K_{(2n_t)1} & K_{(2n_t)2} & \cdots & K_{(2n_t)(2n_t-1)} & K_{(2n_t)(2n_t)} \end{bmatrix} \begin{Bmatrix} u_1 \\ v_1 \\ u_2 \\ v_2 \\ \vdots \\ u_{n_t} \\ v_{n_t} \end{Bmatrix} = \begin{Bmatrix} f_{1x} \\ f_{1y} \\ \vdots \\ f_{Ix} \\ f_{Iy} \\ \vdots \\ f_{n_tx} \\ f_{n_ty} \end{Bmatrix}$$

We obtain

$$\mathbf{K}_{(2n_t)(2n_t)}\mathbf{U}_{(2n_t\times 1)} = \mathbf{F}_{(2n_t\times 1)} \tag{33}$$

Where

$\mathbf{K}_{(2n_t)(2n_t)}$ is the global stiffness matrix for all nt nodes in the entire problem domain,

$\mathbf{U}_{(2n_t\times 1)}$ is the global displacement vector that collect the nodal displacements of all nt nodes in the entire problem domain,

$\mathbf{F}_{(2n_t\times 1)}$ is the global body force vector assembled using the nodal body force vectors for all nodes in the entire problem domain.

4 Numerical Example

In this section, we present a numerical study for elastostatic 2-D problem of a cantilever rectangular homogeneous isotropic plate (Fig.2) [23]. The plate has a unit thickness and E=210.10⁹P, v=0.3, L=54m, D=12m and P=1000N. We consider different numbers of field nodes $n_t = 55, 91, 112$ and 196 nodes that are regularly distributed. Gauss quadrature using 4x4 Gauss points is employed in each background cell.

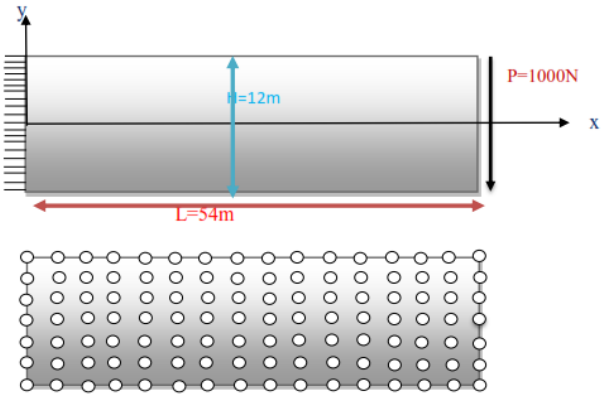

Fg.2: Configuration and nodal arrangement for the cantilever plate

First, we studied the effect of the parameters of the radial basis functions RBF-MQ and the sizes of support and quadrature domain on convergence of the LRPIM method:

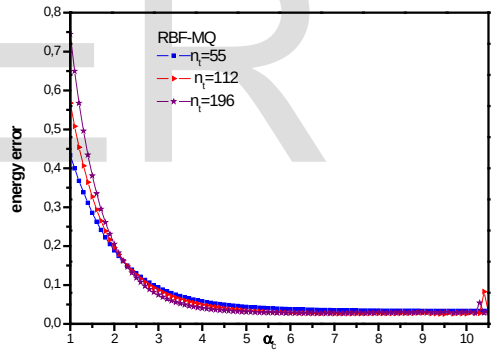

Fg.3: Influence of the shape parameter α_c on the accuracy of the results obtained using RBF-MQ with $\alpha_d = 2.0$, $\alpha_s = 3.4$ and q=2.02

Fig.3 displays the variation of energy error as a function of α_c by the LRPIM methods using RBF-MQ (Table1). We consider different distribution node numbers $n_t = 55, 112$ *and* 196. The results are obtained by using the values of α_d=2.0, q=2.02 and α_s=3.4. We found that all curves fall from maximum value of energy error in α_c=1.0 to the minimum value in α_c=16.8 for $n_t = 55$ or α_c=10.3 for $n_t = 112$ and 196. The domain of convergence is very large and it is between $\alpha_s = 2.5$ and 16.6 for $n_t = 55$ and is between 2.5 and 10.3 for $n_t = 112$ and 196. For the values of α_c greater than 16.8 (for $n_t = 55$), and greater than 10.3 (for $n_t = 112$ and 196), the LRPIM method is not convergent. Note that the domain of convergence is larger than that given by [20].

In fig. 4, shows the variation of energy error as a function of the parameter q of RBF-MQ, for different regular distribution node numbers $n_t = 55, 112, 196$ with following fixed values $\alpha_Q = 2.0$, $\alpha_s = 3.4$ and $\alpha_c = 9.0$. We note in the figure between q=-1.0 and q=0.2 the error decrease gradually, and between 0.2 and 3 the error is steady, but if the value of q is identical to 0.0, 1.0, 2.0 and 3.0 the energy error is very large and the LRPIM method is not convergent. We note that the domain of the convergence is broader than that given in the reference [19].

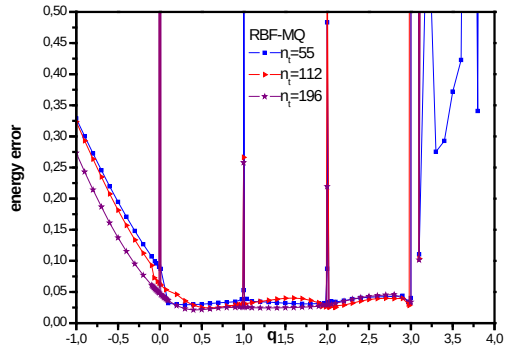

Fg.4: Influence of the shape parameter q on the accuracy of the results obtained using RBF-MQ with $\alpha_Q = 2.0$, $\alpha_c = 9.0$ and $\alpha_s = 3.4$

In fig. 5, the dependence of energy error as a function of the size of the local quadrature domain α_Q for different regular distribution node numbers $n_t = 55, 91, 112, 196$ using radial basis RBF-MQ is investigated. For values ranging between 0.9 and 2.5, the LRPIM method using RBF-MQ is convergent but if the value of $\alpha_Q < 0.9$ or $\alpha_Q > 2.5$, the energy error is very large and the LRPIM method is divergent.

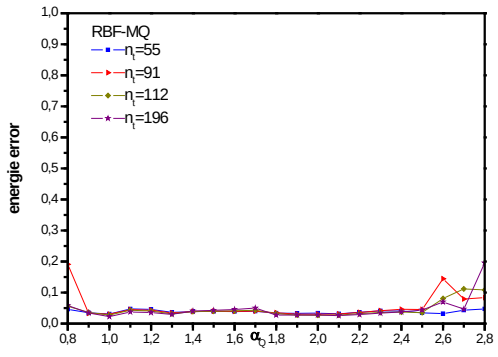

Fg.5: Influence of the shape parameter α_Q on the accuracy of the results obtained using RBF-MQ with $\alpha_c = 6.8$, $\alpha_s = 3.4$ and q=2.02

Fig.6 plots the energy error as a function of the size of the support domain α_S. The result is calculated by the LRPIM method using RBF-MQ and by using the values of $\alpha_Q = 2.0$, q=0.98 and $\alpha_c = 8.0$. It investigated the variation of maximum and minimum values of α_s of convergence domain by using the different distribution node numbers $n_t = 55, 91, 112$ and 196. It can be seen from this figure that if the values of αs is smaller than 1.8, the energy error is large and LRPIM method using RBF-MQ is not convergent. The domain of convergence reaches the maximum value at $\alpha_s = 5.0$ for $n_t = 55$. For greater values of $n_t = 91, 112$ and 196, the domain convergence is smaller than that obtained with $n_t = 55$ and the greater extremity value of the convergence domain is now $\alpha_s = 3.66$. We found a very significant result compared with the result obtained by the reference [21].

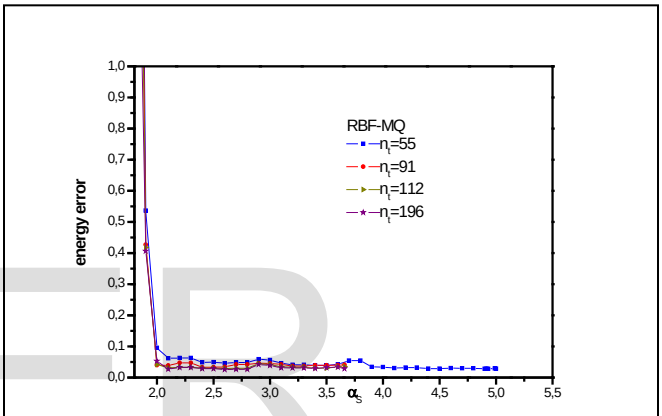

Fg.6: Influence of the shape parameter α_S on the accuracy of the results obtained using RBF-MQ with $\alpha_Q = 2.0$, $\alpha_c = 8.0$ and q=0.98

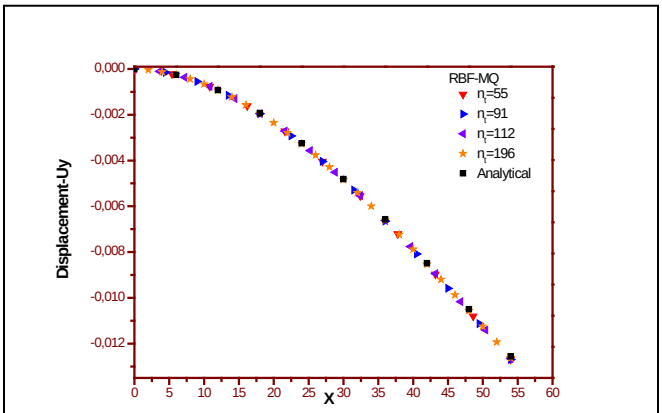

Fg.7: Displacement u_y distribution along the neutral axis with shape parameters q=0.98, $\alpha_c = 8.0$ and $\alpha_s = 3.4$, $\alpha_A = 2.0$

The displacement results as function of x with y =0 are plotted in Fig.7, the fixed values of; size of quadrature domain is

$\alpha_Q = 2.0$ and size of support domain is $\alpha_s = 3.4$. The shape parameters of RBF-MQ are also fixed ($\alpha_c = 8.0$ and q=0.98). The effect of different node numbers on the displacement also presented in this figure. We note that the curves are identical for all node numbers n_t and the shape is identical to that obtained by theoretical analysis (Analytical results).

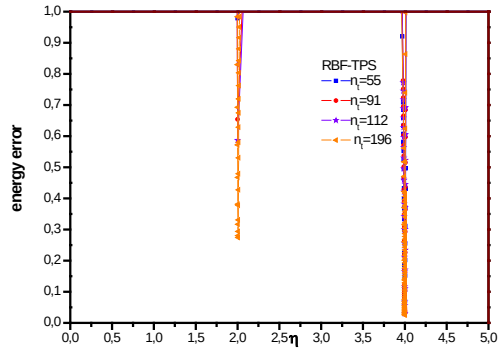

Figure 8: Influence of the shape parameter η on the accuracy of the results obtained using RBF-TPS with $\alpha_Q = 2.0$ and $\alpha_s = 3.0$

We have also used the radial basis function RBF-TPS to study the convergence of LRPIM method:

Fig. 8 displays the variation of the energy error as a function of the shape parameter η for different values of node numbers $n_t = 55, 91, 112$ and 196. The result illustrated in this figure with the radial basis function RBF-TPS gives a domain of convergence very restricted for all different distribution node numbers. In this study, we have considered the single solution value η=4.0001.

Fig.9 illustrates the energy error variation as a function of the size of the support domain α_s for different field node numbers n_t =55, 91, 112, 196. It investigated the variation of maximum and minimum values of α_s of convergence domain. For $n_t = 55$, we note that the energy error value is greater than that obtained by $n_t = 91, 112, 196$. It can also be seen from this figure that if the values of α_s is smaller than 1.8 the energy error is large and LRPIM method is not convergent. The domain of convergence reaches the maximum value at $\alpha_s = 5$ for $n_t = 55$ and for $n_t = 91, 112, 196$ the greater extremity value of the convergence domain is $\alpha_s = 3.66$ and the domain of convergence is smaller than that obtained for $n_t = 55$. The results obtained by the present method are in very good agreement with those obtained in the reference [21].

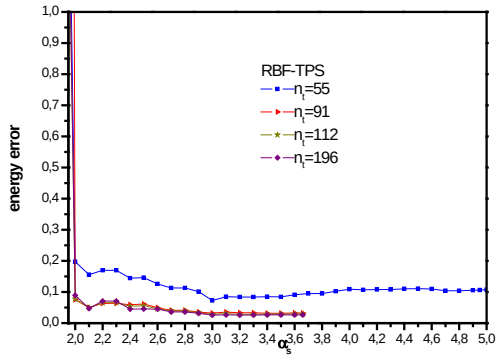

igure 9: Influence of the size of local support domain on the accuracy of the results obtained using RBF-TPS with $\eta = 4.0001$ and $\alpha_Q = 2.0$

Fig.10 gives the variation of the error energy as a function of the size of the local quadrature domain α_Q by LRPIM method using RBF-TPS function with fixed values of shape parameter η=4.0001 and the size of support domain $\alpha_s = 3.0$ for different field node numbers $n_t = 91, 112$ and 196. We can say that the domain of the convergence is larger; it is between 0.6 and 2.7 for $n_t = 91$ and between 0.6 and 3.0 for $n_t = 112$ and 196. We note that if the values of α_Q is smaller than 0.6 or greater than 2.7, the energy error is very high and the LRPIM method is not stable.

Fig. 11, shows the variation of the effective transverse shear stress τ_{xy} as a functions of y with α_s=3.0 and $\alpha_Q = 2.0$ and the shape parameter η =4.0001. The effect of different node numbers on the shear stress distributions on the cross-section at x=L is presented in this Figure; it shows that the accuracy is clear for all node numbers and the shape is identical to that obtained by theoretical analysis (Compared with analytical results).

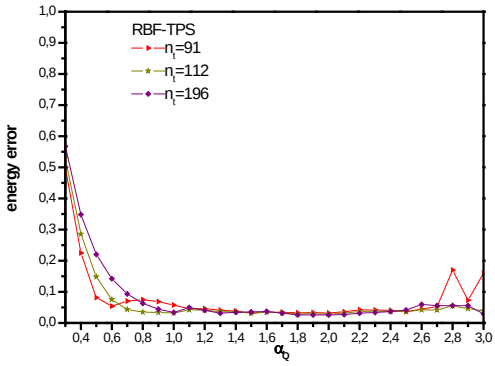

Figure10: Influence of the size of local support domain on the accuracy of the results obtained using RBF-TPS with $\eta = 4.0001$ and $\alpha_s = 3.0$

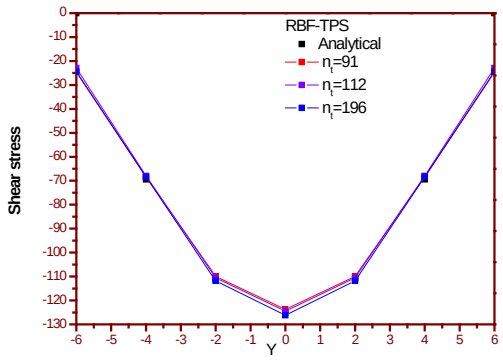

Fig.11: Shear stress distribution along the line of X=L with shape parameter $\eta = 4.0001, \alpha_q = 2.0$ and $\alpha_s = 3.0$

5 Conclusions

In this paper, the Local Radial Point Interpolation Method LRPIM using RBFs functions based on the local residual formulation is developed for solving a 2D elastostatic problem of a cantilever rectangular homogeneous isotropic plate. We studied the optimal shape parameters of RBF-MQ and Thin Plate Spline (RBF-TPS) basis. We also investigated the effect of the dimensionless sizes of the quadrature domain α_q and the support domain αs with different node numbers $n_t = 55, 91, 112$ and 196. We conclude that:

the effect of size parameter αs, for two Radial Basis Functions (RBF-MQ and RBF-TPS) the small values of n_t lead to the upper extremity of convergence domain which is limited to $\alpha_s = 55$; concerning the effect for greater value of n_t, the maximum value diminishes to $\alpha_s = 3.66$.

for the effect of specific parameters, the shape parameters αC and q, the results obtained by using RBF-MQ give a domain of convergence larger than that presented by other authors for α_c and q.

Compared with the analytical results, the LRPIM method produces a very good agreement for stresses and for displacements.

BIBLIOGRAPHY

[1] L. Lucy (1977), a numerical approach to testing the fission hypothesis. *Astron J*. 82:1013–1024.

[2] G. Nayroles, Touzout and P.Villon (1992), generalising the finite element method: diffuse approximation and diffuse elements (DEM), *computational mechanics* 10,307-318.

[3] T. Belytsckho, Y. Lu and L. GU, (1994), Element-Free Galerkin Methods, *International Journal for Numerical Methods in Engineering*, Vol. 37,229-256.

[4] S. N. Atluri, T. Zhu (1998), a new meshless local Petrov–Galerkin (MLPG) approach's in computational mechanics, *Comput. Mech.* 22,117–127.

[5] S. N. Atluri, Shen Shenping (2002), the meshless local Petrov-Galerkin (MLPG) method: a simple & less costly alternative to the finite element and boundary element methods. *Comput. Model. Eng. Sci. 3(1):11–51.*

[6] Y. T Gu., G. R. Liu (2001), a local point interpolation method for static and dynamic analysis of thin beams. *Comput... Meth. Appl. Mech... Eng*. 190: 5515–5528

[7] G. R. Liu, Y. T. Gu (2001), a local radial point interpolation method (LR-PIM) for free vibration analyses of 2-D solids ; *J. of Sound and Vibration* - 246(1), 29-46.

[8] J. G. Wang and G. R. Liu (2000), radial point interpolation method for elastoplastic problems ; Taipei, Taiwan : Proc. of the 1st Int. Conf. *On Structural Stability and Dynamics* - 703-708,2000

[9] G. R. Liu and YT.Gu (2002), A boundary point interpolation method for stress analysis of solids ; *Computational Mechanics* - 47-54 : Vol. 28

[10] [L. HARDY (1971), multiquadric equations of topography and other irregular surfaces. Department of Civil Engineering and Engineering Research Institute Iowa State University, *J. Geophys. Res.;* vol. 76 NO 8: 1905–1915

[11] R. L. Hardy (1990), Theory and applications of the multiquadrics-biharmonic method, *Computers and Mathematics with Applications* vol. 19:163–208.

[12] E. J. KANSA (1990-I), Multiquadrics—a scattered data approximation scheme with applications to computational fluid-dynamics—I. Surface approximations and partial derivative estimates ; *Great Britai : Lawrence Livermore National Laboratory*, L-200, P.O. Box 808, Livermore, CA 94550, U.S.A. - 8/9, pp. 127-145 : Vol. 19.

[13] E. J. KANSA (1990-II), multiquadrics--a scattered data approximation scheme with applications to computational fluid-dynamics--ii solutions to parabolic, hyperbolic and elliptic ; *great britain : lawrence livermore national laboratory*, l-200, p.o. box 808, livermore, ca 94550, u.s.a. - 8/9 pp. 147-161: vol. 19.

[14] J. G. Wang, G.R. Liu (2002), on the optimal shape parameters of radial basis functions used for 2-D meshless methods. *Comput. Meth. Appl. Mech. Eng*. 191. 2611–2630

[15] J. G. Wang and G. R. Liu (2000), radial point interpolation method for elastoplastic problems ; Taipei, Taiwan : Proc. of the 1st Int. Conf. *On Structural Stability and Dynamics* - 703-708,2000

[16] G. R. Liu and Y. T.Gu (2002), a boundary point interpolation method for stress analysis of solids ; *Computational Mechanics* - 47-54 : Vol. 28

[17] Wen Chen, Zhuo-Jia Fu, C. S. Chen (2014), Recent Advances in Radial Basis Function Collocation Methods, *Springer Briefs in Applied Sciences and Technology*, DOI 10.1007/978-3-642-39572-7.

[18] M. J. D. Powell, (1994), the uniform convergence of thin plate splines in two dimensions, *Numerische Mathematic* 68 (1) 107–128

[19] G. R. Liu, L. Yan, J. G. Wang and Y.T. Gu (2002), Point Interpolation Method based on local residual formulation using radial basis functions; *Department of Mechanical and Production Engineering*, November 13 – 6, 713-732 : Vol. 14.

[20] G. R. Liu , G. Y. Zhang , Y. Y. Wang , Z. H. Zhong , G. Y. Li, X. Han (2007), a nodal integration technique for meshfree radial point interpolation method (NI-RPIM), *International Journal of Solids and Structures*, vol. 44:3840–3860.

[21] J. G. Wang and G. R. Liu, (2002), a point interpolation meshless method based on radial basis functions. *Int. J. Number Meth. Eng, vol.*

54 (11): pp. 1623-1648.

[22] L. Victor Shapiro, (1958), the Divergence theorem for discontinuous vector fields, second series *Annals of Mathematics*, Vol. 68, No. 3 (Nov., 1958), pp. 604-624

[23] S. Timoshenko, S. Woinowsky-krieger (1995), Theory of plates and shells. New York: *McGraw Hill, 2nd edition*.